DENTAL MATERIALS 35 (2019) 1017–1030

Available online at www.sciencedirect.com

ScienceDirect

journal homepage: www.intl.elsevierhealth.com/journals/dema

Dentine collagen cross-linking using tiopronin-protected Au/EDC nanoparticles formulations

U. Daood[a], Z. Akram[b], J.P. Matinlinna[c], A.S. Fawzy[d,*]

[a] Clinical Dentistry, Restorative Division, Faculty of Dentistry, International Medical University Kuala Lumpur, 126, Jalan Jalil Perkasa 19, Bukit Jalil, 57000 Bukit Jalil, Wilayah Persekutuan Kuala Lumpur, Malaysia
[b] Department of Periodontology, Faculty of Dentistry, Ziauddin University, Karachi, Pakistan
[c] Dental Materials Science, Applied Oral Sciences, Faculty of Dentistry, The University of Hong Kong, Prince Philip Dental Hospital, 34 Hospital Road, Sai Ying Pun, Hong Kong Special Administrative Region
[d] UWA Dental School, University of Western Australia, 17 Monash Avenue, Nedlands, WA 6009, Australia

ARTICLE INFO

Article history:
Received 23 January 2019
Received in revised form
3 April 2019
Accepted 12 April 2019

Keywords:
Dentin collagen
Biodegradation
Carbodiimides
Nanoparticles
Crosslinking

ABSTRACT

Objective. The aim of this study was to investigate EDC-assisted collagen crosslinking effect with different concentrations of tiopronin-protected gold (TPAu) nanoparticles on demineralized dentine.

Methods. TPAu nanoparticles were fabricated from 0.31-g tetrachloroauric acid and 0.38-g of N-(2-mercaptopropionyl) glycine (2.4-mmol). Then co-dissolved using 35-mL of 6:1 methanol/acetic acid and mixed using $NaBH_4$. EDC (0.3-M) was conjugated to TPAu nanoparticles at TPAU/EDC-0.25:1, and TPAU/EDC-0.5:1 treatment formulations ratios. Dentin specimens treated with 0.3-M EDC solution alone or left untreated were used as control. Nanoparticles formulations were characterized in term of particles morphology and size, Zeta potential, thermogravimetric analysis and small-angle X-ray scattering. Dentin substrates were characterized in term of TEM investigation, dentin proteases characterization, hydroxyproline liberation, elastic modulus measurement, Raman analysis and confocal microscopy viewing.

Results. TEM evaluation of tiopronin protected gold nanoparticles dispersion revealed nanoclusters formations in both groups. However, based on our TEM measurements, the particle-size was ranging from ~20 to 50 nm with spherical core-shape which were almost similar for both TPAu/EDC ratios (0.5:1 and 0.25:1). Zeta potential measurements indicate negative nanoparticles surface charge. SAXS profiles for both formulations, suggest a typical profile for uni-lamellar nanoparticles. Superior dentin collagen cross-linking effect was found with the TPAu/EDC nanoparticles formulations compared to the control and EDC treated groups.

Significance. Cross-linking of dentin collagen using TPAu coupled with EDC through TPAu/EDC nanoparticles formulations is of potential significance in improving the biodegradation resistance, proteases inhibition, mechanical and structural stability of demineralized dentin substrates. In addition, the cross-linking effect is dependent on TPAu/EDC ratio, whereas higher cross-linking effect was found at TPAu/EDC ratio of 0.5:1.

* Corresponding author.
E-mail address: amr.fawzy@uwa.edu.au (A.S. Fawzy).
https://doi.org/10.1016/j.dental.2019.04.005

1. Introduction

Long term adhesion is a direct result of stability and integrity of collagen fibers within resin–dentine hybrid layer [1]. Fibrillar collagen network forms the organic framework of dentine which accounts for approximately 90% of the organic dentine matrix [2]. Endogenous enzymes present within dentine and hybrid layer are known to cause degradation via hydrolysis of collagen fibers which are not completely enveloped by polymerized adhesive [3]. Failure of adhesive layer leads to formation of micro gaps readily penetrated by pathogens [4]. This degradation has been minimized over time by application of different strategies including reinforcement of collagen fibers within resin-dentine hybrid layer [5], deactivation of endogenous enzymes [6,7], and or within a combination of both [8].

Dentine bonding is a continuously challenging clinical field. Inspired by the important role of cross-linking in tissue function [9], extensive efforts have been made to optimize collagen matrix inducing exogenous cross-linking [10,11]. It is widely understood that additional cross-links will prevent collagen molecules from sliding past each other [12] and thereby increasing mechanical strength and considerably increasing stiffness [13], tensile strength and compressive strength [14]. Intermolecular cross-links improve resistance of collagen to enzymatic degradation by masking the cleavage site of collagen [15]. Enzymatic modifications include formation of pyridinium and pyrrolic molecules within the N-(NTX) and C-terminal telopeptides (ICTP and CTX). They are initiated by the oxidation of lysine and hydroxylysine residues that are catalyzed by the enzyme lysyl oxidase [16]. Increased intermolecular cross-links within collagen structure prevents unravelling of the fibrillar collagen structure and restricts the α-chains' degree of freedom by masking the cleavage site of collagen. This will, further resist it against enzymatic degradation due to matrix-bound matrix metalloproteinases and cysteine cathepsins [17]. Some cross-linkers induce collagen cross-linking by actively replacing collagen bound water by reducing the hydrophilicity of acid-etched demineralized dentine surface and thereby promoting adhesive infiltration [18].

Cross-linking methods mostly used incorporate a bridge molecule as a part of the cross-link moiety. There is formation of covalent cross-links (bonds) produced as a result of exogenous cross-links (carbodiimide, grape seed, glutraldehyde and riboflavin) which inactivate dentine proteases by blocking MMP active sites. These endogenous proteases within dentine matrices can be inactivated by application of cross-linkers for as little as 1 min [19]. In addition, zero-length linkers are used as coupling agents, such as EDC, 1-ethyl-3-(3-dimethyl aminopropyl) carbodiimide, capable of forming peptide bonds [20]. Structural changes are manifested due to pyridinoline cross-link providing a three-way connection, which are three side groups of collagens connected together [21]. A dendrimer [22] with 4, 8, and 16 amino groups was cross-linked to collagen using EDC, producing thermal stability in case of collagen molecules and gels with potential applications and effective carriers for different small molecule deliveries. This also enables different cross-links and multiple cross over functionalities that are possible [23,24]. In addition, the application of EDC to acid-etched dentine helps in maintaining the viscoelasticity of the resin–dentine hybrid layers [25]. EDC has shown lowest collagen degradation [26] in terms of mass loss and release of telopeptides, against specimens pretreated in alkaline media [27]. As mentioned above, formation of peptide bonds within the amino groups of collagen molecules is comprehensively achieved by EDC.

Collagen fibers, when treated with gold nanoparticles, result in 2D assemblies [28]. There is a guided electrostatic attraction between the nanoparticle and collagen fibers due to spatial arrangement of these assemblies [29]. Gold nanoparticles have been widely used to enhance the performance by using favorable properties associated with reduced size of the material [30]. Even so, gold nanoparticles can be easily functionalized with biological macromolecules as they are biologically inert and have no direct effect on the molecular structure [31]. This allows additional area and greater number of reactions to occur at the surface of material [32]. For this we have devised a novel approach using tiopronin-modified (trade name 'Thiola', 2-(2-sulfanylpropanoylamino) acetic acid) gold nanoparticles to assist in dentine collagen cross-linking. Au-nanoparticles are known to form various cross-links with collagen due to the presence of multiple carboxyl groups (−COOH) on the surface in the presence of EDC [24]. The application of Au-nanoparticles as a cross-linking agent has allowed for multiple and easy incorporation of biomolecules including peptides, by immobilization at the Au surface [33]. That said, the aim of the current laboratory study was to investigate the potential synergetic collagen crosslinking effect of EDC when conjugated with tiopronin-protected Au-nanoparticles (TPAu) on demineralized dentine substrate at different ratios of TPAu/EDC. The null hypotheses tested were: (i) the conjugation of TPAu with 0.3 M EDC; and (ii) the different ratios of TPAu/EDC (0.25:1 and 0.5:1) have no effect on collagen crosslinking, biodegradation resistance, endogenous proteases expression and mechanical properties of demineralized dentine substrate. Our current study also presents a multi-disciplinary research in order to obtain a complete characterization of the formulation used as a novel approach over demineralized dentine substrate.

2. Materials and methods

2.1. *Nanoparticles synthesis and characterization*

2.1.1. *Chemicals*

2-Mercaptopropionylglycine (tiopronin, 99%, also called: 2-(2-sulfanylpropanoylamino) acetic acid), sodium borohydride ($NaBH_4$; 99%) and other chemicals were purchased from Sigma Aldrich. All chemicals were of reagent grade and were used as received without purification.

2.1.2. *TPAu nanoparticles synthesis*

Using 0.31 g tetrachloroauric acid ($HAuCl_4$; 0.80 mmol) and 0.38 g of 2-mercaptopropionylglycine (2.4 mmol), a solution was dissolved using 35 mL of 6:1 methanol/acetic acid. The solution produced a ruby red colour and it was further mixed with $NaBH_4$ (0.6 g, 16 mmol) in 15 mL of distilled H_2O using a rapid stirrer in a beaker. This was performed via increasing temperature between 24 °C to 44 °C in 20 min. While

pH of the solution was slowly increased to 5.1 from 1.28, the suspension was eventually stirred for 40 min and cooled removing the solvent under vacuum at ≤45 °C. Available tiopronin was completely insoluble in methanol and purified using dialysis dissolving in 80 mL of NANO pure water (Merck Millipore) with dropwise inclusion of HCL, maintaining pH to 1. Crude tiopronin-gold (TPAu) solution was slowly stirred with recharging with fresh water every 10 h over the course of 72 h. Tiopronin was removed from the dialysis tubes and solvent evaporated at ≤45 °C [34,35].

2.1.3. *EDC conjugation with TPAu nanoparticles*

Fifty milliliters of a stirred 2 mM aqueous solution TPAu was titrated with 2 mM NaOH and was dissolved in 30 mg/mL of distilled water (Millipore) with the pH of the resultant solution maintained to $\tilde{7}$. TPAu nanoparticles were conjugated with EDC, at different ratios, before being applied to dentine collagen substrates. EDC (0.3 M) was added to the TPAu nanoparticles solution at different ratios and left overnight under continuous stirring in a horizontal shaker set to 200 rpm to allow a complete mixing. The final concentration of EDC to the tiopronin-protected gold particles was maintained at ratios of: TPAu/EDC-0.25:1, TPAu/EDC-0.5:1.

2.1.4. *Transmission electron microscopy characterization of nanoparticles*

Formvar (polyvinyl formal) coated copper grids (200 mesh) were used onto which 1 mg/mL aqueous solution was dropped, allowed to collect for 5 min. Excess solution was removed by using a small piece of filter paper touching at the edge of the copper grids. For further drying, the grids were kept under N_2 flow for 15 min. The phase contrast images of the nanoparticles were obtained using a Philips CM 200 electron microscope working at 200 kV. Three randomly selected regions of each specimen were obtained at 340,000x with size distribution using Scion Image Beta Release 2 (Scion Corporation, Frederick, Md).

2.1.5. *Zeta potential measurements*

Zeta (ζ) potential of prepared nanoparticles was recorded by photon correlation spectroscopy using a Zetasizer 3000 HAS (Malvern Instruments, Germany). Nanoparticles (300 μL) with different ratios, TPAu/EDC-0.25:1, and TPAu/EDC-0.5:1, were mixed with 4 mL of Millipore water immediately before measuring their zeta potential at room temperature. The viscosity of water and refractive index were used for calculation of the results. Thermogravimetric Analysis (TGA), synchrotron small angle X-ray scattering (SAXS) and TPAu/EDC Application to Demineralized Dentine were analysed and the methodology and results presented in the supplemental data.

2.1.6. *TPAu/EDC application to demineralized dentine*

Extracted caries-free human molars (n = 86) were collected after the patients' informed consent and was approved by the Institutional Review Board. After disinfection, occlusal enamel was removed using a slow speed saw under water irrigation to expose the mid-coronal dentine (Isomet, Buhler, Lake Bluff, IL, USA). Dentine specimens were cut (dimensions and shapes vary according to the testing procedure indicated below) using low speed diamond saw, cleaned in distilled water, demineralized using 10 wt% phosphoric acid (H_3PO_4) for 24 h, rinsed with distilled water for 15 s, and then air-dried.

Dentine specimens were randomly distributed between the different control and experimental groups. In the first group (control), no treatment with TPAu/EDC or EDC alone was done, and the demineralized dentine specimens subjected to 50 μL of deionized water for 1 min. In the second, third and fourth groups, after excess water was removed with absorbent paper leaving the dentine surface in hydrated condition, each specimen was treated with 50 μL of their respective modification solutions (EDC, TPAu/EDC-0.25:1 and TPAu/EDC-0.5:1 respectively) for 1 min, and finally rinsed gently with deionized water for 30 s.

2.2. *TEM characterization of demineralized dentine collagen structure*

TEM characterization of demineralized dentine discs (0.5 ± 0.1 mm thick and 4 mm diameter) was done to study structural variations of dentine collagen matrix and similar dentine discs (n = 5) were used, with or without nanoparticles modification, after storage in artificial saliva (AS) modified with collagenase (100 μm/L) Type-I (AS/Col) for 3 months [36]. After storage, specimens were gently rinsed for 5 min, fixed, buffered with 0.1 M sodium cacodylate for 1 h, treated by 1% osmium tetroxide (OsO_4) in phosphate buffered solution (PBS) for 1 h, rinsed with distilled water, dehydrated in ascending concentrations ethanol, and finally followed by infiltration with araldite resin. Ultra-microtome with a diamond knife was used to cut ultrathin sections ($\tilde{9}$0 nm) from and collected on the grids and stained with uranyl-acetate, $UO_2(CH7COO)_2{\cdot}2H_2O$, for 10 min before TEM imaging at 100 KV (JEOL-1010, Japan).

2.3. *Mechanical characterization of the demineralized dentine beams*

Mechanical testing was performed to evaluate the apparent elastic modulus (E_{app}) of demineralized dentine beams having the dimensions of 0.5 mm thickness × 1.7 mm width × 6.5 mm. The dentine beams (n = 13) divided into the four control and experimental groups and tested after 1week storage in the artificial saliva modified with collagenase solution (As/Col). Three-point bending testing was done at 2.5 mm span-length with a displacement rate of 0.5 mm min^{-1} using a universal testing machine (Instron, 5848 Microtester, USA) in hydrated condition. The apparent elastic modulus (E_{app}) was calculated as previously described [12].

2.4. *Analysis of dentine proteases*

Dentine beams were then prepared with dimensions of 6 mm × 2 mm × 1 mm (a total of 40 beams). After demineralization in 10 wt% H_3PO_4 at 25 °C for 24 h, beams were later rinsed with deionized water with constant stirring at 4 °C for 1 h [37,28]. Dentine beams were randomly allocated to four groups (n = 10), treated as previously described, blot dried and placed in individually labelled propylene tubes with 1 mL calcium and zinc containing media (CM) at 37 °C for 7, 14 days, or 1-month in a shaking-water bath (Thermo Fisher Scientific) for

60 cycles/min [38]. After each incubation time period demineralized dentine beam were rinsed with 10 mL distilled water at 4 °C, blot dried and placed in a desiccator for 3 days. Dry mass at each time point was measured to the nearest 0.001 mg using an analytical balance (XP6 Microbalance, Mettler Toledo, Hightstown, NJ, USA). After dry mass measurement, beams were rehydrated in deionized water at 4 °C for 1 h before treatment with designated disinfectants. The medium obtained after each incubation period was stored in a freezer (−80 °C) and subsequently analyzed for C-terminal cross-linked telopeptide (ICTP) and C-terminal peptide (CTX) fragments. Amount of solubilized type I collagen ICTP fragments using an ICTP enzyme-linked immunosorbent assay (ELISA) kit (UniQ EIA, Orion Diagnostica, Espoo, Finland). Collagen matrix degradation activity of cathepsin K was determined by measuring the amount of CTX fragments within the incubation medium, using a Serum Crosslaps ELISA kit (Immunodiagnostic System, Farmington, UK).

For direct protease detection in demineralized dentine specimens, dentine powder was prepared using the same protocol as mentioned previously. Five 1-g aliquots of dentine powder were demineralized. Demineralized dentine powder was rinsed with deionized water for 5 times, dried and divided into the four study groups (n = 7). Extraction buffer (r [50 mM Tris−HCl at pH 7.5 containing 0.2% Triton X-100, 5 mM $CaCl_2$, and 100 mM NaCl]) was used to re-suspend treated dentine powder for 24 h to extract the proteases. Vials were centrifuged at 20,000 rpm at 4 °C for 30 min. Supernatants were collected, dialyzed in bags with 30 kDa molecular cut-off overnight, lyophilized and frozen at −20 °C until they were analyzed using ELISA (Human MMP2 ELISA Kit – Lot #5619 for MMP-2; Human CTSK/Cathepsin K ELISA Kit – Lot #5614 for cathepsin K, both from Lifespan Biosciences, Seattle, WA, USA) in triplicates expressed as ng/mL.

2.5. Collagenase mediated collagen resistance to degradation

Hydroxyproline (HYP) content in supernatant was measured at 48 h in collagenase using an assay kit (BioVision, Exton, PA, USA). Dentine slabs (4.5 mm × 3.5 mm × 0.5 mm) were prepared, demineralized in phosphoric acid, randomly distributed between the four groups (n = 7) and treated as described above. HCl (12 M) were used to hydrolyze 100 μL aliquots at 120 °C for 3 h. From the 100 μL aliquots, 10-μL quantities were transferred to a 96-well plate for evaporation under vacuum and Chloramine-T buffer reagent (100 μL) added, and solutions incubated at 27 °C for 5 min. 100 μL of DMAB reagent was added later, incubated for 90 min at 60 °C and absorbance measured using a spectrophotometer (Ultramark; Bio-Rad, Hercules, CA, USA) at 560 nm [39].

2.6. Raman spectroscopy

Phosphoric acid demineralized dentine discs (1 mm) from each group (n = 5) were used for Raman analysis. For Raman spectroscopy and data acquisition, spectral analyses were obtained from 5 points randomly distributed over the surface per each dentine disc using a Raman system (Renishaw InVia Raman microscope), with $\tilde{2}\ cm^{-1}$ spectral resolution and 830 nm laser source (Renishaw Plc, Wotton-under-Edge, UK). Each spectrum was collected for 5 s at an average of 10 spectra focusing the laser beam randomly onto a $\tilde{2.5}$ μm spot on each specimen (20× objective; NA = 0.40). A polynomial fitting algorithm was used for background fluorescence removal. For sub-peak identification, $\tilde{1}670–1640\ cm^{-1}$, $\tilde{1}670–1690\ cm^{-1}$, and $\tilde{1}670–1610\ cm^{-1}$ of original Amide I intensities (normalized to $\nu1PO_4$ at $\tilde{9}60\ cm^{-1}$) were directly calculated. In addition to this, following ratios of peak intensities were also calculated; hydroxyproline/proline ratio (at $\tilde{8}77\ cm^{-1}$ per Pro at $\tilde{8}55\ cm^{-1}$ or at $922\ cm^{-1}$) for post-translational modifications after crosslinking; mineral-to-matrix ratio ($\nu1PO_4$ at $\tilde{9}60\ cm^{-1}$ per proline at $\tilde{8}55\ cm^{-1}$, $\nu1PO_4$ per Amide III at $\tilde{1}247\ cm^{-1}$ and $\nu1PO_4$ per Amide I at $\tilde{1}668\ cm^{-1}$) as a measurement of mineralization.

2.7. Confocal imaging

Confocal laser scanning system (Axioplan 200, Carl Zeiss MicroImaging, Jena, Germany) was used for visualization within the visible light spectrum. Laser wavelength of 514 nm (argon, 15 mW) was used in multi-tracking mode to excite the luminescence of Au-nanoparticles delivered within demineralized dentine disc specimens ($n = 3$), within fixed spectral bands [40]. Image variation had an image detection offset of −0.02 and a main beam splitter of 80/20. After focusing on the specimen images were taken at six different spots. Focus of Au nanoparticles were adjusted using the differential interference contrast as reference.

2.8. Macrophage isolation and analysis

Human peripheral blood mononuclear cell line, SC (BPS, Bioscience, Inc., San Diego, USA) CRL-9855 #LOT: 61834527, ATCC) at a concentration of 2×10^5 cells was maintained in a flask. Cells were counted using Iscove's Modified Dulbecco's Media (IMDM; ATCC, Lot 63331110-Manassas/Vancouver, and 1×10^6 cells/mL cultured supplemented with 10% FBS, 0.05 mM 2-mercaptoethanol (2-sulfanylethan-1-ol) 0.1 mM hypoxanthine and 0.016 mM thymidine. Resting macrophages (Mθ), were generated with induction of lipopolysaccharide (LPS-PG ultrapure *Porphyromonas gingivalis*-TLR4 ligand; 0.1 μg/mL) after 6 h and added over with interferon gamma (IFNγ, 20 ng/mL) using the same protocol from Daood and Yiu [41]. The wells were than incubated for another 66 h. On the third day, cells were pretreated with crosslinking formulations: devoid of treatment (control); EDC 0.3 M; TPAu/EDC-0.25:1, and TPAu/EDC-0.5:1 for 2 min (inside medium). After removing IMDM medium, the cells were washed with PBS and immunofluorescence staining performed on dentine substrate with primary antibodies of CD68+, CD80+ (M1 profile), and CD163+ (M2 profile) respectively. After washing with PBS, DAPI (Vectashield; Catalog #H-1200-Vector Laboratories, 4′,6-diamidino-2-phenylindole) was added for analysis of blue fluorescence for few specimens. On top, the coverslips were mounted onto the glass slides for CLSM (Fluoview FV 1000, Olympus, Tokyo, Japan) analysis, which was performed under dark, and macrophages imaged on a confocal microscope using light emission between 500–550 nm with an excitation wavelength of 488 nm at 40x objective lens for direct observa-

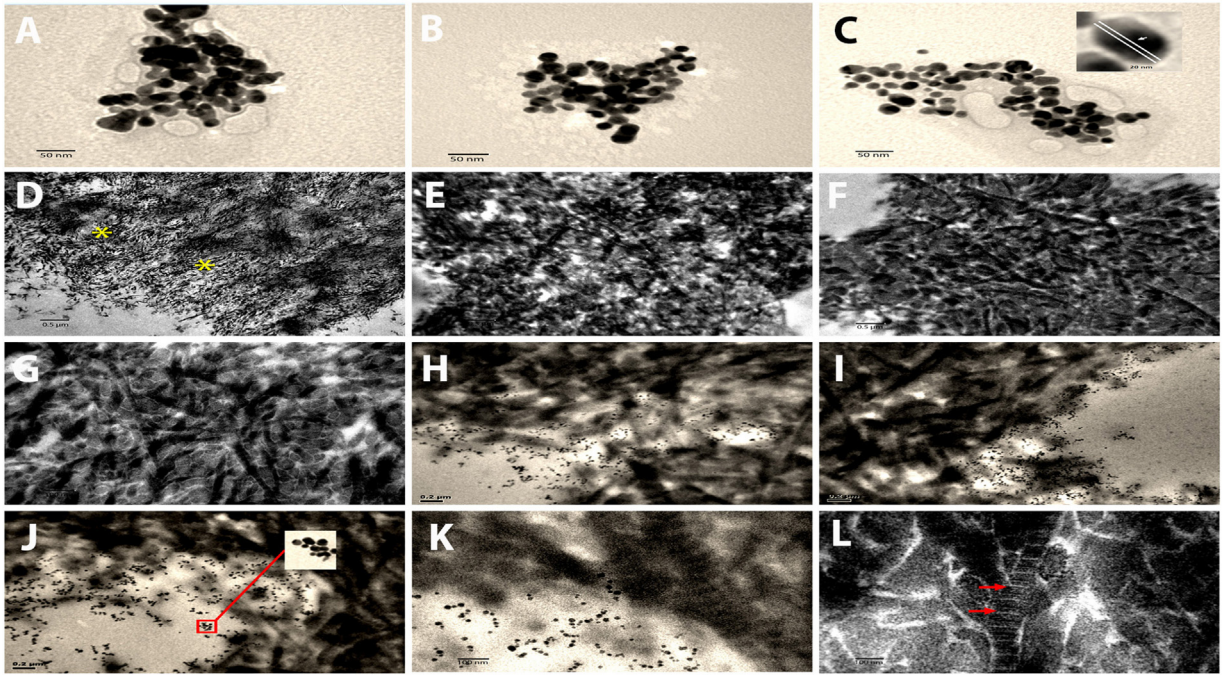

Fig. 1 – Representative TEM images showing the morphology of (A) TPAu/EDC-0.25:1 and (B–C) TPAu/EDC-0.5:1 nanoparticles formulations. All nanoparticles exhibited uniform spherical shape and showed a tendency to be clustered together with a few separate nanoparticles. High-magnification TEM image (inset C) revealed the spherical structure of the TPAu/EDC-0.5:1 nanoparticle. (D) TEM micrograph of collagen fibers after enzymatic degradation showing presence of denatured collagen fibers resembling a moth-eaten appearance (yellow *) with frayed edges. (E) The EDC 0.3 M cross-linked specimens showed disrupted fibrillar arrangement with unclear cross banding. The TPAu/EDC-0.25:1 treated specimens showed dense fibrillar arrangement and slightly normal cross-banding of the fibers (F). TPAu/EDC-0.5:1 treated specimens resulted in fibrillar arrangement and well-maintained collagen architecture (G). (H–I) TEM image showing presence of the TPAu/EDC-0.25:1 and TPAu/EDC-0.5:1 nano particles inside the dentinal tubules of the demineralized dentine specimens respectively. TPAu/EDC-0.5:1 nanoparticle are seen to penetrate inside the dentinal tubules (inset red box is high magnification of nanoparticle cluster) (J). (K) Higher magnification of dentine specimens treated with TPAu/EDC-0.5:1 showed preservation of the well-formed collagen fibril structure. (L) Absence of fibril decomposition in TPAu/EDC-0.5:1 specimen. Arrows (I) point to well-maintained cross-banding, on normal sized thick-fibers.

tion. Percentages of M1 and M2 were determined by dividing CD80+ (M1) and CD163+ (M2) by the number of CD68+ cells in each field tested [42]. An M1/M2 ratio was then calculated (Eq. (1)) for each specimen as follows:

$$M1/M2 = percent\ M1\ cells/percent\ M2\ cells \quad (1)$$

2.9. Statistical analyses

Generally, data were presented as mean ± standard deviation and analyzed by one-way ANOVA followed with the Tukey's multiple post hoc comparison test using SPSS (SPSS v20, SPSS, Chicago, IL, USA). P values $p < 0.05$ considered statistically significant. Percentage of M1 and M2 cells was determined by dividing CD80 (M1) and CD163 (M2) by the number of CD68 cells in each field tested. Values were analyzed using one-way ANOVA ($\alpha < 0.05$) with the Tukey's multiple post hoc comparison test. Using SPSS (v20, SPSS, Chicago, IL, USA), data reflecting pixel numbers were analyzed using the Holm–Sidak pair-wise multiple test ($p < 0.05$). For HYP liberation, data were expressed as means ± standard deviations and analyzed by one-way ANOVA followed by the Tukey's post hoc test for repeated-measurement comparison as $p < 0.05$ was considered statistically significant. Using normality (the Kolmogorov–Smirnov test) and homoscedasticity (the modified Levene's test), percentage of dry mass loss and ICTP (ng telopeptide/mg dry dentine) and CTX (pg telopep-tide/mg dry dentine) were analyzed. When the normality and equality variance assumptions of data were validated, they were analyzed using repeated measures ANOVA along with post hoc multiple comparisons using the Tukey's test. Data for Raman analysis are presented as mean ± SD and parameters and assessed by the nonparametric Kruskal–Wallis test. This was followed by the Dunn's correction including multiple comparisons ($p < 0.05$). Raman intensities between control and other experimental groups were analyzed using the Mann–Whitney test as a function of wavenumbers within Raman change.

3. Results

3.1. TEM analysis

A series of contrast images of nanoparticles were taken at various magnifications (Fig. 1A–C). The limited contrast between

Table 1 – Mean (±SD) for inhibition of MMP-2 and cathepsin K activities (ng/mL) obtained with Human MMP-2 and cathepsin K ELISA Kit system. Mean (±SD) of apparent elastic modulus (E_{app}) in MPa of demineralized dentine. Mean (±SD) of Zeta potential (mV) of the two TPAu/EDC nanoparticles formulations. Groups identified by different superscripts letter are statistically significantly different within each column.

Groups	MMP-2	Cathepsin	E_{app}	Zeta potential (mV)
Control	8.81 (3.11) ^{A}	5.50 (4.10) ^{A}	3.22 (3.20) ^{A}	
EDC 0.3M	6.17 (2.70) ^{B}	3.41 (2.70) ^{B}	5.11 (1.40) ^{B}	
TPAu/EDC-0.25:1	2.81 (1.70) ^{C}	1.88 (1.22) ^{C}	7.40 (2.19) ^{C}	−21.4 (5.1) ^{A}
TPAu/EDC-0.5:1	1.93 (2.50) ^{D}	0.34 (1.99) ^{D}	9.60 (3.10) ^{D}	−37.2 (4.2) ^{B}

the background and nanoparticles was one of the pivotal difficulties while assessing particle size as discussed in subsequent section. TPAu/EDC-0.25:1 (Fig. 1A) and TPAu/EDC-0.5:1 (Fig. 1B–C) specimens showed spherical shaped nanoparticles clusters having size-range of 20–50 nm with no difference in appearance was noted between the two groups.

For dentine specimens, TEM micrographs from control group (Fig. 1D) revealed a collagen matrix that contained non-intact collagen fibers indicating a significant degradation effect of collagenase. There was also a clear increase in interfibrillar space demonstrating an irregular contour. The 0.3 M EDC treated specimens (Fig. 1E) showed an increased number of fibers in a relatively uniform manner when compared to the control specimens. In addition, specimens were clearly containing partially deteriorated collagen fibers or components. The experimental TPAu/EDC-0.25:1 (Fig. 1F) and TPAu/EDC-0.5:1 (Fig. 1G) groups were indicative of denser and smoother arrangements of collagen fibers which were thicker and regularly arranged with intact cross-banding forming more organized network structures. The TEM investigation confirmed deep delivery and close association/attachment of TPAu/EDC nanoparticles (Fig. 1H–J) in non-clustered forms around collagen fibers and inside the dentinal tubules. High magnification imaging confirmed the intact collagen structure with the associated TPAu/EDC-0.5:1 nanoparticle (Fig. 1K) even after the 3 months' storage in the artificial saliva/collagenase solution (Fig. 1L) where collagen fibers preserved their characteristic D-periodic banding pattern, and the micro-fibrillar structure.

3.2. *Characterization of nanoparticles and adsorption of TPAu/EDC nanoparticles to demineralized dentine*

Surface charges of TPAu/EDC (for both experimental groups) are listed in Table 1. Zeta potential measurements indicate negative surface charge for both of TPAu/EDC-0.25:1 (−37.5 ± 4.2) and TPAu/EDC-0.5:1 (−21.4 ± 5.1) nanoparticles.

3.3. *Analyses of dentine proteases and HYP*

The loss of dry mass, release of CTX and ICTP over a period of 7 and 14 days, and one month is shown in Fig. 2. Dentine beams that were treated with TPAu/EDC-0.25:1 ($\tilde{}$ −7.120 ± 2.57, $\tilde{}$ −14.56 ± 3.48, $\tilde{}$ −12.34 ± 5.51 for 7 and 14 days and one month) and TPAu/EDC-0.5:1 ($\tilde{}$ −4.11 ± 2.57, $\tilde{}$ −6.44 ± 3.86, $\tilde{}$ −3.86 ± 6.51 for 7 and 14 days and one month) showed the least amount of dry mass loss as compared to the control group (Fig. 2A). Both the factors of incubation time and the cross-linking formulation used and the interaction factor between them had a significant effect on loss of dry mass for the experimental groups ($p < 0.001$). The percentage of dry mass loss for both TPAu/EDC-0.25:1 and TPAu/EDC-0.5:1 groups for 7 and 14 days remained not significantly different ($p < 0.001$). However, the changes were significantly different after one month within their own respective groups and when compared to other EDC and control groups. The dry mass was observed as highest amongst the control group after one month (Fig. 2A).

Release of CTX generated by cathepsin K was significantly decreased for all cross-linker pretreatment groups ($p < 0.001$) after all time periods, compared to the untreated control groups (Fig. 2B). Both factors, cross-linkers and time, had a significant effect on CTX release and the interaction of the two factors was also significant ($p < 0.001$). After one month of incubation, the CTX release was significantly reduced in TPAu/EDC-0.5:1 group, instead of an increase. The percentage of CTX release was significantly lower in experimental groups compared to untreated control after 7, 14 days and one month ($p < 0.001$). No significant difference in CTX release was observed within the TPAu/EDC experimental groups at 7 and 14 days ($p < 0.05$). ICTP telopeptide showed a similar trend with all experimental groups showing significant differences in all time periods when compared to the control group ($p < 0.001$). There was a higher ICTP release in the first seven days for EDC groups ($\tilde{1}4.22 \pm 1.86$), which gradually decreased ($\tilde{4}.11 \pm 1.51$) after one month (Fig. 2C). Control beams that were not treated by any cross-linker released $\tilde{2}0.73 \pm 2.80$ ng ICTP telopeptides/mg dry dentine after 1 month of incubation in a complete medium (Fig. 2D). The lowest ICTP values were recorded in beams treated with experimental TPAu/EDC-0.5:1 groups followed by TPAu/EDC-0.5:1. In all treated groups, a low level of ICTP was detected in the incubation medium, even though significantly less loss of dry mass was observed after one month of incubation.

Concentrations of the tested active enzymes present in the experimental treated nanoparticle groups were significantly lower (Table 1) than the ones tested against the control and EDC groups (<0.05). There was a significant difference between the control and EDC groups in the concentration of MMP-2 and cathepsin K. The TPAu/EDC-0.5:1 group had the least MMP-2 and cathepsin K release from demineralized dentine specimens when compared to experimental EDC and TPAu/EDC-0.25:1 groups.

In groups TPAu/EDC-0.25:1 and TPAu/EDC-0.5:1 cross-linking significantly decreased ($p < 0.05$) the HYP liberation compared with the non-cross-linked and EDC specimens at the 48-h time-point (Fig. 2E). No difference was found in HYP liberation between TPAu/EDC-0.25:1 and TPAu/EDC-0.5:1 groups.

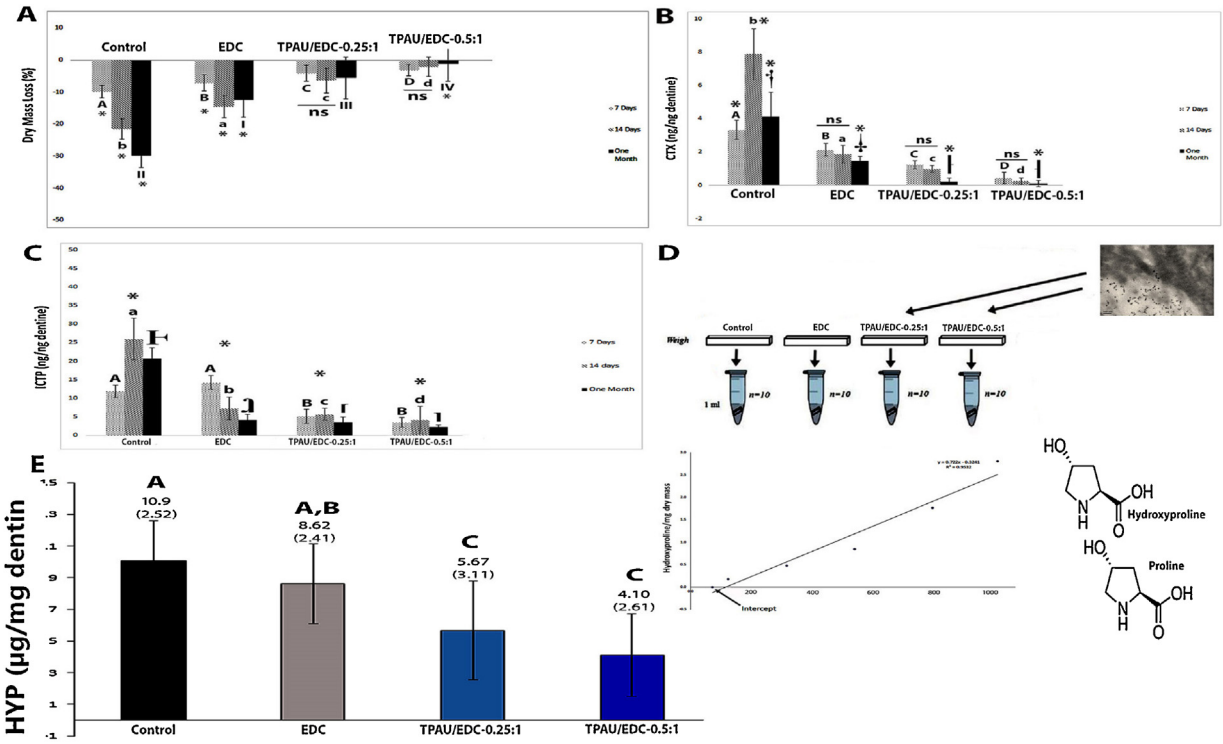

Fig. 2 – (A) Cumulative loss of dry mass from demineralized dentine beams pretreated with cross-linkers up to one-month in the incubation medium. Values are means and standard deviations of the percentage dry mass loss (n = 10). The loss of dry mass from each beam was calculated as a percentage of the original dry mass of that beam at baseline. (B) The amount of CTX telopeptides released per ng/mg dentine from various treatment groups at 7th day/14th day/one-month in the incubation medium. (C) The amount of ICTP telopeptides released per ng/mg dentine from various treatment groups at 7th day/14th day/one-month in the incubation medium. Values are means and standard deviations for all analysis done (n = 10). *: significant difference groups. Uppercase/lowercase letters/numerals/symbols represent differences between each pre-treatment (7th day/14th day/one-month) ($p < 0.001$); ns: no significant difference. (D) Schematic representation of beams subjected to different or no cross-linking treatment ($p < 0.001$); (E) Hydroxyproline (HYP) release from solubilized collagen peptide fragments in incubation medium for 48 h. Values are µg HYP/mg as heights of bars are means; error bars indicate ± SD (n = 10). Groups identified by different letters are significantly different ($p < 0.05$); Insert: Regression analysis.

3.4. *Mechanical characterization*

A progressive and statistically significant increases in stiffness (Eapp) were observed in TPAu/EDC-0.25:1 and TPAu/EDC-0.5:1 groups ($p < 0.05$) compared to the other groups (Table 1). The lowest stiffness value was observed for the control group (nonmodified demineralized dentine) when compared to EDC and gold nanoparticle treated demineralized dentine specimens.

3.5. *Raman analyses*

Comparing average Raman spectra across groups per crosslinking methods (Table 2), there were significant changes in hydroxyproline, crystallinity and carbonate signals when treated with TPAu/EDC-0.5:1. The TPAu/EDC-0.5:1 specimens showed intensity values which were higher as compared to controls and the TPAu/EDC-0.25:1 specimen, except the carbonate and ν_1PO_4/Amide I parameters. Effects of EDC can be isolated for ν_1PO_4/Amide I, ν_1PO_4/Amide III, and ν_1PO_4/CH_2 which showed lower changes with significant changes when compared to controls. TPAu/EDC-0.25:1 specimens showed no significant differences except for the carbonate parameter when compared to control (Table 2).

The Amide I and Amide III peaks appeared as strong organic Raman signal peaks and were not affected by noise within the spectrum as compared to other Raman peaks. Based on the analysis, the Amide III peaks were seen slightly shifted to different locations at $\tilde{1}237\ cm^{-1}$, $\tilde{1}243\ cm^{-1}$, $\tilde{1}245\ cm^{-1}$ and $\tilde{1}246\ cm^{-1}$ for control, EDC, TPAu/EDC-0.25:1 and TPAu/EDC-0.5:1 specimen respectively (Fig. 3B). These peaks were seen to be sensitive to the type of cross-linking method used distinguishing different intensities amongst the experimental groups for both TPAu groups with TPAu/EDC-0.5:1 showing the highest intensity. A difference in intensity between TPAu groups were identified as $5\ cm^{-1}$. For the Amide I changes (Fig. 3C), and as expected for the crosslinking methods applied, the associated Amide III peaks showed changes amongst the spectra with a difference in intensity also seen between control and their respective cross-linked experimental groups. The acquired Raman spectra were control $\tilde{1}678\ cm^{-1}$>, EDC $\tilde{1}676\ cm^{-1}$>, TPAu/EDC-0.25:1 $\tilde{1}669\ cm^{-1}$>, TPAu/EDC-0.5:1 $\tilde{1}665\ cm^{-1}$. The Raman spectra of experimental groups compared to control groups showed that intensities

Table 2 – Comparison of Raman parameters of control, EDC and TPAu/EDC nanoparticles treated dentine specimens with significant *p*-values 0.001.

Parametrics	Wavenumber cm^{-1}	Value	Control	EDC	TPAu/EDC-0.25:1	TPAu/EDC-0.5:1
Raman parameters	Hyp/Pro	877 cm^{-1}–855 cm^{-1}	0.68 ± 0.01 vs control	0.66 ± 0.03	0.76 ± 0.05	0.81 ± 0.02
			n.sig.	*n.sig.*	$p < 0.000$	
	Crystallinity	1/FWHM (ν_1PO_4)	0.086 ± 0.003 vs control	0.093 ± 0.005	0.074 ± 0.002	0.065 ± 0.002
			n.sig.	*n.sig.*	$p < 0.000$	
	Mineral/matrix	ν_1PO_4/amide I	31.36 ± 2.12 vs control	22.34 ± 3.33	26.77 ± 2.61	29.91 ± 4.1
			$p < 0.000$	*n.sig.*	*n.sig.*	
		ν_1PO_4/amide III	16.64 ± 0.54 vs control	13.12 ± 1.11	14.50 ± 0.79	16.11 ± 1.89
			$p < 0.000$	*n.sig.*	*n.sig.*	
		ν_1PO_4/CH_2 wagging	14.11 ± 0.79 vs control	11.33 ± 2.33	13.10 ± 2.79	15.22 ± 2.77
			$p < 0.000$	*n.sig.*	*n.sig.*	
	Carbonate	CO_3/ν_1PO_4	0.147 ± 0.004 vs control	0.139 ± 0.004	0.178 ± 0.003	0.165 ± 0.001
			n.sig.	$p < 0.000$	$p < 0.000$	

Key: *n.sig.* = not significant.

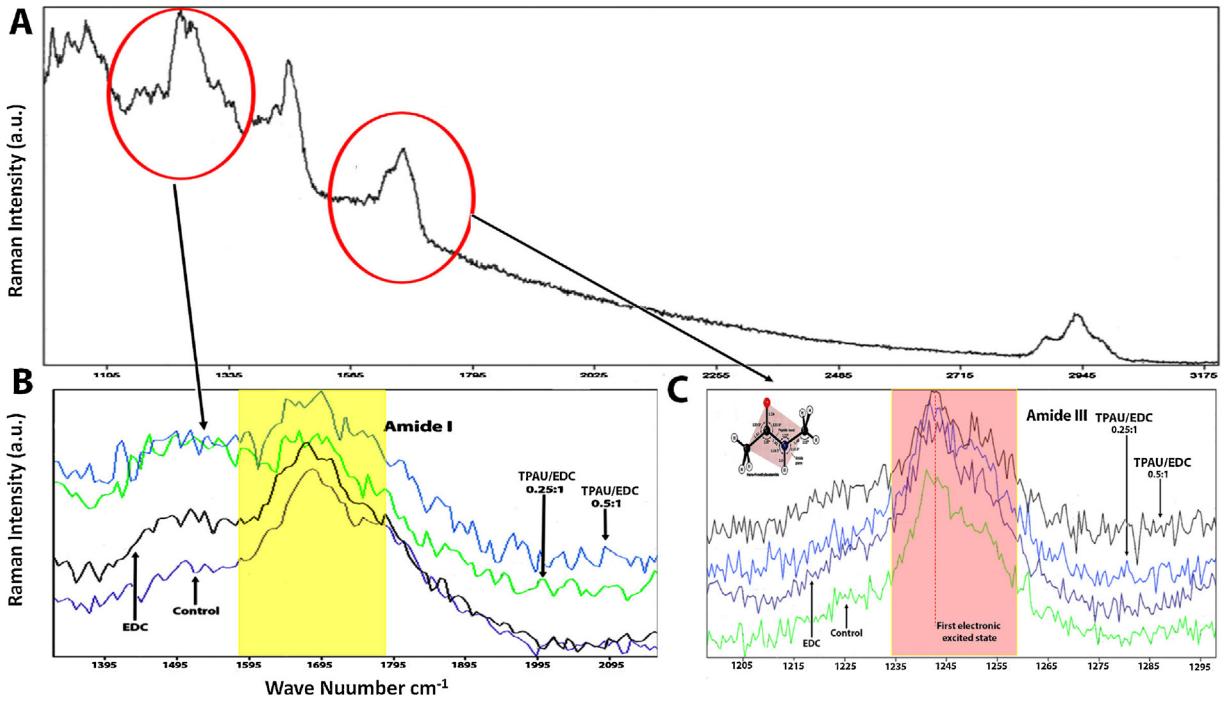

Fig. 3 – (A) Average Raman spectra from 1100 cm^{-1} to 3000 cm^{-1} of dentine; (B–C) TPAu/EDC-0.25:1 and TPAu/EDC-0.5:1 treated dentine showing different spectra (Amide I and III; C–H bonds of organic content) respectively visualizing spectral contributions of organic matrix and collagen after treatment with different groups. Both Amide I and III bands show higher intensities for specimens treated with TPAu/EDC-0.25:1 and TPAu/EDC-0.5:1 experimental groups when compared to control and EDC.

at the wavenumber locations of the Amide III and Amide I associated peaks decreased and increased respectively.

3.6. *Confocal microscopy*

Representative images taken for TPAu/EDC-0.25:1 and TPAu/EDC-0.5:1 groups are shown in Fig. 4. The appearing irregular arrays of pixels reflected a probable Brownian motion of diffusing particles. However, some of the particles did not appear fixed on dentine. The box plots represent the median with 35 and 65% quartiles of reflecting pixels in each of the TPAu/EDC-0.25:1 and TPAu/EDC-0.5:1 experimental groups, respectively, after excitation at $\lambda = 514$ nm. There was no reflection of control samples, while others showed

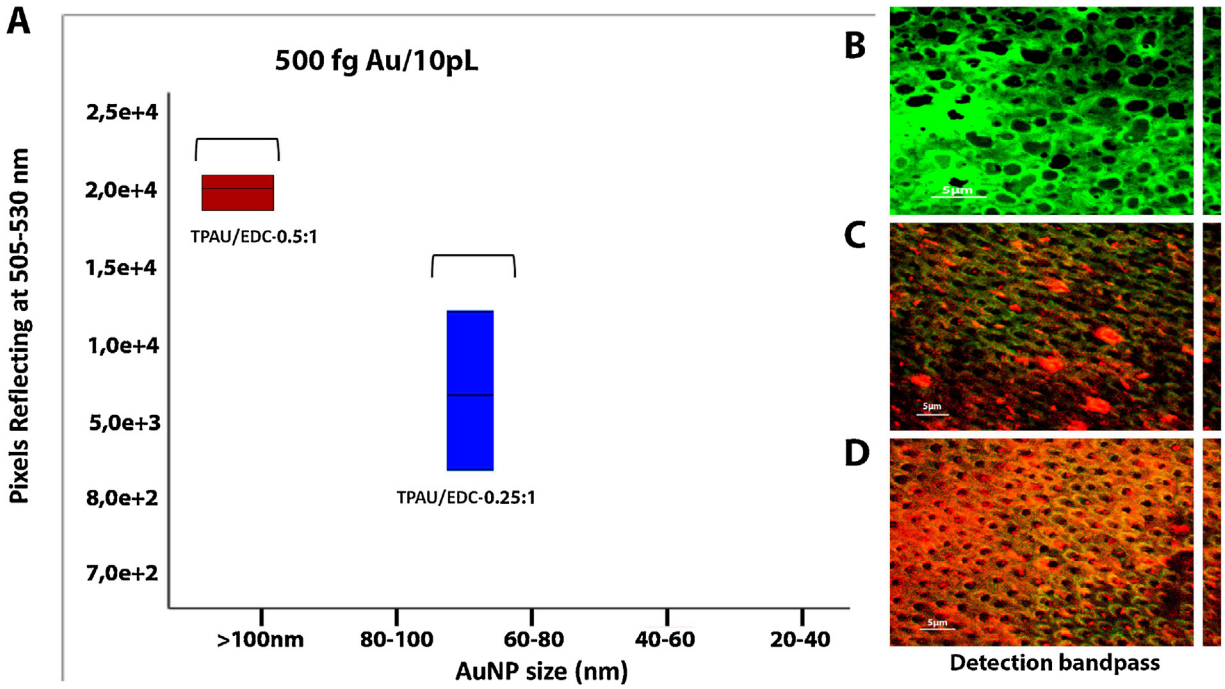

Fig. 4 – Representative images of (A) confocal intensities of different groups (B) control; (C) TPAu/EDC-0.25:1 and (D) TPAu/EDC-0.5:1 in 10-pL volumes. Size of TPAu/EDC-0.25:1 was ~100 nm. Excitation was performed at λ = 514 nm. The box plots represent the median with quartils of reflecting pixels after excitation at 514 nm.

reflection of excitation wavelengths in the TPAu/EDC-0.25:1 and TPAu/EDC-0.5:1 groups. That said, data from excitation at λ = 514 nm accounted for the highest number of reflection due to the proximity to the reflection of gold in TPAu/EDC-0.5:1 group.

3.7. *Macrophage phenotype*

The M1/M2 macrophage ratios after application of different cross-linking solution showing a distribution of macrophages to analyze for the different subtypes of macrophages are shown in Fig. 5. The results of one-way ANOVA showed that M1/M2 ratio (Fig. 5A) was significantly reduced in TPAu/EDC-0.25:1 and TPAu/EDC-0.5:1 groups, when compared to control, and EDC groups ($p < 0.001$). An M1 type response (pro-inflammatory) is indicative when values are above 1.0 while values less than 1.0 are considered an M2 type response (anti-inflammatory). Mononuclear macrophages of CD68+ (in absence of induction) were present in all cells when observed in confocal analysis (Fig. 5B–D). Macrophage cells treated with TPAu/EDC-0.25:1 (Fig. 5B) and which were stained with DAPI show nuclei of cells for total cell observation. Moreover, the image using confocal microscopy confirmed the cellular components. Staining showed a clear presence of macrophages (data not shown for TPAu/EDC-0.25:1). In a qualitative analysis of phenotype of macrophages, cells were predominantly CD163+ in the TPAu/EDC-0.25:1 (Fig. 5C) and TPAu/EDC-0.5:1 groups (Fig. 5D, indicative of M2 markers. Conversely, the CD80+ markers were also found in the EDC groups (Fig. 5A inward) as the CD80+ and CD163+ markers distinguish between different macrophages. With double immune-fluorescent staining and confocal analysis, these markers to a large extent separate between two different cellular populations.

4. Discussion

Amongst the strategies for dentine collagen crosslinking, one such approach involves the use of cross-linking agents [43–46]. That said, using functionalized nanoparticles for collagen cross-linking is a newly adopted approach for reinforcing collagen tissues by binding directly to collagen side-chain moieties. Moreover, cross-linking of functional nanoparticles to collagen may optimize its physico-chemical and biological properties [47]. After bonding with biological molecules such as collagen, nanoparticle surface changes cause a change in the refractive index, making use of nanoparticles, such as gold nanoparticles, feasible for utilizing biomolecule interactions. Use of such multiple-way cross-linkers result in development of novel materials exhibiting unique, optimized properties [48]. These exciting findings also open new avenues in application of nanoparticle-based strategies for cross-linking collagen for dental applications. Since most of collagen crosslinking involve a two-point link between collagen molecules, in the current study we have deployed TPAu as a connecting (or linking) agent because of its ability to form more than two bonds with collagen biomolecules.

The principle of this study is based on tiopronin-protected gold nanoparticles (TPAu) are cross-linked to dentine only through carbodiimide coupling such as EDC with average formation of up to eight amide-bonds for each particle with collagen lysine/hydroxylysine moieties [49–51]. Accordingly,

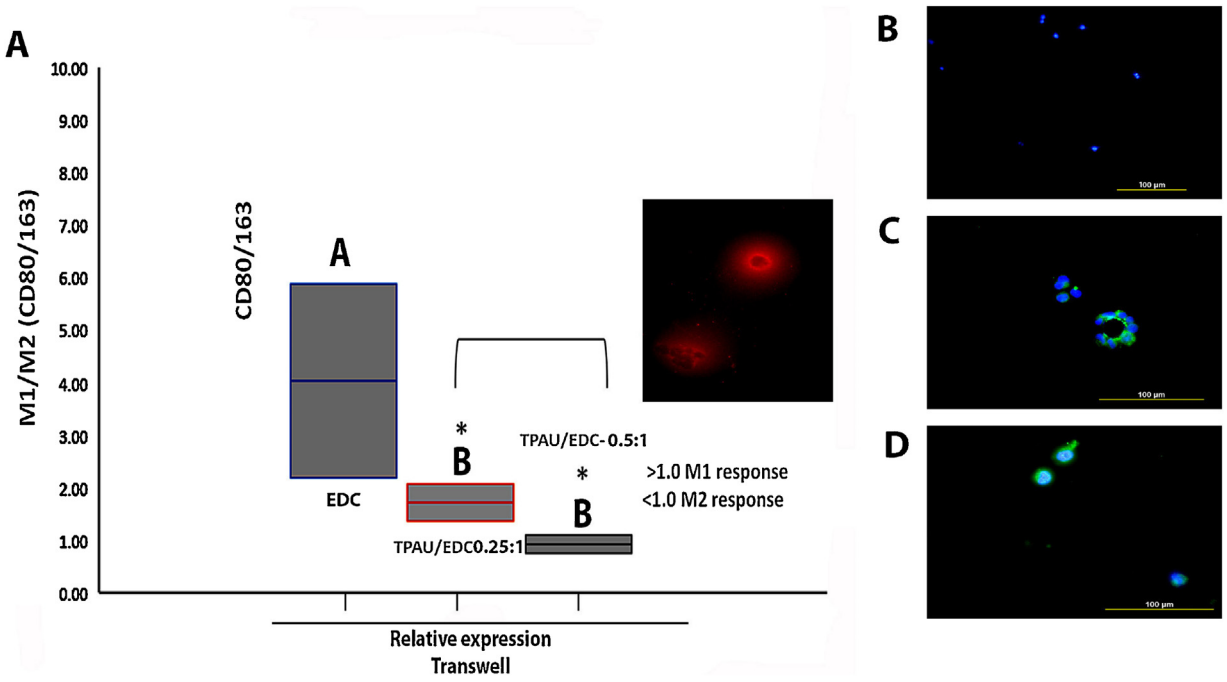

Fig. 5 – (A) Ratio of the percentage of M1/M2 macrophages after application of different cross-linkers. Values above 1.0 are indicative of an M1 type response while values less than 1.0 are indicative of an M2 type response. CD80+ and CD 163+ distinguish between macrophage phenotypes. Confocal images of immuno fluorescence staining in (B) DAPI staining for specimens treated with TPAu/EDC-0.25:1; Nuclei are clearly revealed by DAPI staining (blue), and overlay is fluorescence collected by all channels; (C–D) TPAu/EDC-0.5:1. CD163+ and CD80 + positive cells were detected in both TPAU/EDC-0.25:1 (data not shown) and TPAu/EDC-0.5:1 groups. Specimens of Dapi (4′,6-diamidino-2-phenylindoleblue), CD163+ (green), and CD80+ (red). Scale bar = 100 μm.

two experimental formulations having ratios of TPAu/EDC-0.25:1 and TPAu/EDC-0.5:1 were investigated in this study. Based on the results of this study, the null hypotheses should be rejected as superior dentine collagen cross-linking effect was found with the TPAu/EDC nanoparticles formulations compared to the control and EDC treated groups. The superior cross-linking effect found with the TPAu/EDC nanoparticles formulations could be generally attributed and explained based on cross-linking of collagen with TPAu was performed via the EDC carbodiimide coupling reaction with the formation of amide bonds between each TPAu particle and collagen lysine moieties as explained in detail below.

The TPAu nanoparticles were synthesized according to a protocol mentioned previously [49]. We have analyzed TEM images by measuring the diameter of nanoparticles (Fig. 1A–C). TEM evaluation of tiopronin protected gold nanoparticles dispersion revealed nano-clusters formations in both groups. However, based on our TEM measurements, the particle-size was ranging from ~20 to 50 nm with spherical core-shape which were almost similar for both TPAu/EDC ratios (0.5:1 and 0.25:1) due to similar estimated tiopronin groups are present on Au nanoparticles surface.

It is known that cross-linking can be evaluated on basis of loss of free amino groups during the cross-linking process as Au nanoparticles attach to only one lysine group [50]. Cross-linking carried out via EDC alone can result only in ~2.3% loss of amino groups which seems to be engaged in inter and intramolecular cross-linking of collagen [51]. It is speculated that the TPAu ratios with EDC used may have enabled the majority of free amino groups be utilized in formation of bonds. This could have resulted in increased cross-linking density between collagen carboxyl groups and nanoparticles/EDC. Even so, this resulting higher cross-linking intensity was visible in high magnification TEM of TPAu/EDC-0.5:1 experimental groups. It is well known that amino acids may prefer to bind to nanoparticles with a specific diameter through their anionic group or an aromatic group [52]. Average mass of Type I collagen molecule is 300 kDa and the average number of cross-links present on each nanoparticle is 7.9 ± 0.4 [53]. That said, it does appear that the new TPAu/EDC nanoparticles formulation provides multiple porosities and linkers that can explain the structure of the actual nanoparticle. By looking at the TEM (Fig. 1) and Raman (Fig. 3) analyses, we can assume that all amino moieties present in collagen showed a stable collagen structure with cross-banding seen in TPAu/EDC groups. The experimental groups TPAu/EDC-0.25:1 and TPAu/EDC-0.5:1 appeared very similar and may have caused the same amount of collagen cross-links. The nanoparticle formulation had achieved deep nanoparticle delivery and infiltration inside the dentinal and lateral tubules (Fig. 1H–K). These nanoclusters formed were facilitated through the dentinal tubules of demineralized dentine. Presence of water or electrostatic attraction inside demineralized dentine may have facilitated nanoparticles delivery and infiltration [54]. The quantification of nanoparticles inside dentinal tubules was not done at this stage of the study.

TEM analysis of dentine matrix, from the control group, after degradation (Fig. 1D) revealed dispersed collagen fibers showing irregularities, of different shapes and complete loss of alternate light and dark bands. The resulting collagen fibers appear to be having a crimped appearance with loss of D-banding pattern maintaining a very loose alignment with the thin fibrillar arrangement. After cross-linking with the TPAu/EDC formulations, there was dense collagen packing and the appearance of D-bands seen amongst demineralized dentine sections with uniform diameters (Fig. 1F & G). These are a characteristic fingerprint of the fibrous collagen and on the basis of these correlated images, regions of fibril alignment could be identified. In addition, TEM investigation supported the synergetic effect of TPAu/EDC nanoparticles formulations compared to using EDC alone (Fig. 1E).

Dentine protease analysis showed that our novel collagen cross-linking nanoparticles formulations can act as good inhibitor of cathepsin-K and MMP activities in demineralized dentine matrices. The effect on MMP activities is generally considered source dependent and is highly variable [55]. In order to see a longer effect, the current study was investigated for one month and the results clearly suggested that the hypothesis (i.e. different ratios of tiopronin protected Au gold nanoparticles have no effect on endogenous proteases extracted from dentine) can be rejected. Control specimens had shown an increased loss of dry mass compared to other experimental groups. Interestingly, same trends were observed in our recent study [56], as MMP-2 attack C-terminal telopeptides while MMP-8 can cleave triple helical part of collagen into ¾ N-terminal and¼ C-terminal of collagen [57]. However, in exogenous cross-linker groups, proteases may have been inactivated resulting in lesser loss of dry mass, with least results recorded for TPAu/EDC-0.5:1 groups (-1.22 ± 5.36). As mentioned above, when it has been suggested that TPAu ratios with EDC used may have utilized majority of free amino groups, they may have been causing increasing cross-linking density. Nevertheless, this increasing cross-linking restricts the degree of freedom of its α-chains and prevents unraveling of collagen microfibrillar arrangement. Release of CTX telopeptides showed similar trends for all groups. One interpretation for this result is that the accessibility for EDC with TPAu/EDC groups was more and with passage of time, when peptides are cleaved, release is limited. One-month CTX release in all pretreatment groups was significantly ($p < 0.05$) lower than in control group. Treatment of the demineralized dentine matrix with TPAu/EDC cross-linking formulations significantly reduced the 1-month release of ICTP, which was more pronounced with TPAu/EDC-0.5:1 group (Fig. 2C). The fact that nanoparticles based cross-linking treatment groups did not release any more ICTP could be interpreted as an indication of sustained cross-linking effect. EDC inactivated proteases in pretreatment media as 0.3-M EDC forces reaction of matrix-free carboxylic acids in collagen and endogenous proteases to form activated carboxyl groups that spontaneously react with free amino groups to form amide-type matrix bonds [58]. The effect was stronger when compared to TPAu/EDC groups indicating that the conjugation of EDC with TPAu nanoparticles has an important role on both the subsequent solubility of dentine matrix and on the degree of inactivation of MMPs and cathepsin K. However, this estimation may carry along some errors associated with dispersion of nanoparticles. In the current study, the two TPAu/EDC formulations had inhibited endogenous proteases. This said, it was found that TPAu/EDC-0.25:1 and TPAu/EDC-0.5:1 can be considered as minimum thresholds that had significantly reduced MMP activities, also effecting the modulus of elasticity (Table 1) of dentine ($p < 0.05$) and some other dentine properties. Nevertheless, the results require the rejection of null hypothesis that tiopronin protected Au gold nanoparticles have no effect on mechanical properties of dentine substrate and will improve biomechanical properties.

It is noteworthy that HYP release is due to degradation of collagen based to collagenase enzymes such as cysteine and cathepsins [59]. HYP assay is considered non-specific, and this can indicate tissue collagen concentration [60]. Accordingly, lower HYP release found with experimental TPAu/EDC cross-linking might indicate a higher collagen content and resistance of demineralized dentine matrix to bacterial collagenase-mediated collagen degradation. This effect could be further explained with micro-Raman results. A representative Raman spectrum of TPAu/EDC groups versus control group were compared (Fig. 5). In both spectra, there was clear indication of major contributions of protein-based Raman signals with clear and identifiable bands seen at Amide I and Amide III regions with striking difference seen between the TPAu/EDC groups and other groups. The Amide I band correlates to the secondary structure of the proteins, [61] predominantly the α-helix mode centered around 1645–1650 cm^{-1} [62]. The Amide I band depicts stretching carbonyl (=CO) vibrations while the Amide III is the NH plane deformation along with CN-stretching. These shifts, which are at higher intensities in the TPAu/EDC groups, are primarily due to sensitivity and secondary changes in polypeptide chains. Therefore, these spectral changes may have showed changes due to the degree of cross-linking effect. Triple helical structure and its stability is achieved by formation of peptide bonds within and between collagen chains. Furthermore, collagen Type-I triple-helical domains have an amino acid sequence (primary structure) that, in addition to glycines, is rich in hydroxyproline and proline, which impart rigidity and stability to collagen triple-helical domain [63]. The decrease and increase of Raman shifts and intensities in the Amide I and III regions can be interpreted and attributed to the formation of stable cross-links within collagen network indicating the penetrative effect of TPAu/EDC modification. The HYP/Pro ratio was considered as an indicator of Type I collagen changes as a result of enzymatic processing of proline (proline residue hydroxylation). The TPAu/EDC-0.5:1 groups showed significant changes compared to control along with changes in crystallinity (Table 2). This is primarily due to a slight supramolecular rearrangement which was detected by Raman spectrometry, causing a sensitive response to HYP than to proline, leading to an increase in intensity of hydroxyproline peak, relative to proline peak (data not shown). Similarly, an increase in the mineral/matrix ratio was inversely associated with increase in mechanical properties of the substrate detected [64]. Even so, in our current study, the ratio increased with use of TPAu/EDC-0.5:1 formulation, suggesting an increase in mechanical properties. This is indicative also for the three-point bending test and it is also reject-

ing the first null hypothesis that 'tiopronin protected Au gold nanoparticles have no effect on mechanical properties of dentine substrate'. This might be possibly due to the increase in the matrix-maturity ratio [65]. On the other hand, the observed Raman peak changes do not indicate direct changes to the secondary collagen. This aspect merits further research in the near future.

Confocal microscopic visualization shows patches of TPAu/EDC-0.25:1 and TPAu/EDC-0.25:1 nanoparticles appearing bigger than 100 nm sized particles and being rather from 70 nm to 80 nm respectively. This is probably reflecting the size difference providing massive reflective spots on both specimens. From Au nanoparticles smaller than 20 nm, no reflection could be recorded. Perhaps interestingly, all these findings result in a rather continuous spread of particles in TPAu/EDC-0.25:1 specimen. In addition, the present study also examined the effects of TPAu/EDC formulations on the macrophage phenotype, which can be identified and differentiated according to the cell surface markers, cytokine and gene expression markers [66]. The M1 and M2 reactions are involved in early or late inflammatory and tissue remodeling phases respectively [67]. The CD 80+ identifies M1-activated cells and CD163+ show high expression in M2-activated macrophages. Any imbalances seen in the ratios can increase or decrease chronic inflammatory conditions. Application of both TPAu/EDC groups shifts the polarization profile of macrophages to anti-inflammatory or M2 phenotype profile indicating tissue repair and regeneration. These findings suggest normal regulation of M1–M2—and a cross-linking strategy that is biocompatible.

5. Conclusion

In summary, cross-linking of dentine collagen using TPAu coupled with EDC through TPAu/EDC nanoparticles formulations is of potential significance in improving the biodegradation resistance, proteases inhibition, mechanical and structural stability of demineralized dentine substrates. In addition, the cross-linking effect is dependent on TPAu/EDC ratio, whereas higher cross-linking effect was found at TPAu/EDC ratio of 0.5:1.

Acknowledgements

This work was supported, in part, by grant PG10402012 University of Western Australia. The authors thank the labs at Nanocat University of Malaya, School of Dentistry at International Medical University Kuala Lumpur and Biomaterials-Tissue Engineering Lab at University of Malaya for the research experiments and analysis.

Appendix A. Supplementary data

Supplementary material related to this article can be found, in the online version, at doi:https://doi.org/10.1016/j.dental.2019.04.005.

REFERENCES

[1] Liu Y, Tjäderhane L, Breschi L, Mazzoni A, Li N, Mao J, et al. Limitations in bonding to dentin and experimental strategies to prevent bond degradation. J Dent Res 2011;90:953–68.
[2] Kinney J, Marshall GJ, Marshall S. Three-dimensional mapping of mineral densities in carious dentin: theory and method. Scanning Microsc 1994;8:197–204.
[3] Mazzoni A, Pashley DH, Nishitani Y, Breschi L, Mannello F, Tjäderhane L, et al. Reactivation of inactivated endogenous proteolytic activities in phosphoric acid-etched dentine by etch-and-rinse adhesives. Biomaterials 2006;27:4470–6.
[4] Bourbia M, Ma M, Cvitkovitch DG, Santerre JP, Finer Y. Cariogenic bacteria degrade dental resin composites and adhesives. J Dent Res 2013;92:989–94.
[5] Breschi L, Mazzoni A, Ruggeri A, Cadenaro M, Di Lenarda R, De Stefano, et al. Dental adhesion review: aging and stability of the bonded interface. Dent Mater 2008;24:90–101.
[6] Mazzoni A, Scaffa P, Carrilho M, Tjäderhane L, Di Lenarda R, Polimeni A, et al. Effects of etch-and-rinse and self-etch adhesives on dentin MMP-2 and MMP-9. J Dent Res 2013;92:82–6.
[7] Daood U, Yiu CK, Niu LN, Tay FR. Effect of a novel quaternary ammonium silane on dentin protease activities. J Dent 2017;58:19–27.
[8] Daood U, Tsoi JKH, Neelakantan P, Matinlinna JP, Omar HAK, Al-Nablusi M, Fawzy AS. In vitro assessment of ribose modified two-step etch-and-rinse dentine adhesive. Dent Mater 2018;34(8):1175–87.
[9] Stefano V, Torsello B, Bianchi C, Cifola I, Mangano E, Bovo G, et al. Major action of endogenous lysyl oxidase in clear cell renal cell carcinoma progression and collagen stiffness revealed by primary cell cultures. Am J Pathol 2016;186:2473–85.
[10] Daood U, Swee Heng C, Neo Chiew Lian J, Fawzy AS. In vitro analysis of riboflavin-modified, experimental, two-step etch-and-rinse dentin adhesive: Fourier transform infrared spectroscopy and micro-Raman studies. Int J Oral Sci 2015;7:110–24.
[11] Fawzy AS, Nitisusanta L, Iqbal K, Daood U, Beng LT, Neo J. Characterization of riboflavin-modified dentin collagen matrix. J Dent Res 2012;91:1049–54.
[12] Bailey AJ, Light ND, Atkins ED. Chemical cross-linking restrictions on models for the molecular organization of the collagen fibre. Nature 1980;288:408–10.
[13] Dias J, Diakonis VF, Lorenzo M, Gonzalez F, Porras K, Douglas S, et al. Corneal stromal elasticity and viscoelasticity assessed by atomic force microscopy after different cross linking protocols. Exp Eye Res 2015;138:1–5.
[14] Chen YC, Chen M, Gaffney EA, Brown CP. Effect of crosslinking in cartilage-like collagen microstructures. J Mech Behav Biomed Mater 2017;66:138–43.
[15] Fawzy AS, Nitisusanta L, Iqbal K, Daood U, Neo J. Riboflavin as a dentin crosslinking agent: Ultraviolet A versus blue light. Dent Mater 2012;28(12):1284–91.
[16] Patrick G. The contribution of collagen crosslinks to bone strength. Bonekey Rep 2012;182:1–8.
[17] Aldahlawi NH, Hayes S, O'Brart DP, Akhbanbetova A, Littlechild SL, Meek KM. Enzymatic resistance of corneas crosslinked using riboflavin in conjunction with low energy, high energy, and pulsed UVA irradiation modes. Investig Ophthalmol Vis Sci 2016;57:1547–52.
[18] Moreira MA, Souza NO, Sousa RS, Freitas DQ, Lemos MV, De Paula DM, et al. Efficacy of new natural biomodification agents from Anacardiaceae extracts on dentin collagen cross-linking. Dent Mater 2017;33:1103–9.

[19] Seseogullari-Dirihan R, Apollonio F, Mazzoni A, Tjaderhane L, Pashley DH, Breschi L, et al. Use of crosslinkers to inactivate dentin MMPs. Dent Mater 2016;32:423–32.
[20] Gratzer PF, Lee JM. Control of pH alters the type of cross-linking produced by 1-ethyl-3-(3-dimethylaminopropyl)-carbodiimide (EDC) treatment of acellular matrix vascular grafts. Biomed Mater Res 2001;58:172–9.
[21] Henkel W, Glanville RW, Greifendorf D. Characterization of a type-I collagen trimeric cross-linked peptide from aorta and its cross-linked structure. Detection of pyridinoline by time of-flight secondary ion-mass spectroscopy and evidence for a new cross-link. Eur J Biochem 1987;165:427–36.
[22] Matinlinna JP, Lassila LVJ, Kangasniemi I, Yli-Urpo A, Vallittu PK. Shear bond strength of Bis-GMA resin and methacrylated dendrimer resins on silanized titanium substrate. Dent Mater 2005;21:287–96.
[23] De Paoli Lacerda SH, Inqber B, Rosenzweig N. Structure-release rate correlation in collagen gels containing fluorescent drug analog. Biomaterials 2005;26:7164–72.
[24] Duan X, Sheardown H. Crosslinking of collagen with dendrimers. J Biomed Mater Res A 2005;75:510–8.
[25] Zhang Z, Mutluay M, Tezvergil-Mutluay A, Tay FR, Pashely DH, Arola D. Effects of EDC crosslinking on the stiffness of dentin hybrid layers evaluated by nanoDMA over time. Dent Mater 2017;33(8):904–14.
[26] Turco G, Frassetto A, Fontanive L, Mazzoni A, Cadenaro M, Di Lenarda, et al. Occlusal loading and cross-linking effects on dentin collagen degradation in physiological conditions. Dent Mater 2016;32(February 2):192–9.
[27] Seseogullari-Dirihan R, Mutluay MM, Tjaderhane L, Breschi L, Pashely DH, Tezvergil-Mutluay A. Effect of pH on dentin protease inactivation by carbodiimide. Eur J Oral Sci 2017;125(4):288–93.
[28] Whelove OE, Cozad MJ, Lee BD, Sengupta S, Bachman SL, Ramshaw BJ. Development and in vitro studies of a polyethylene terephthalate-gold nanoparticle scaffold for improved biocompatibility. J Biomed Mater Res B Appl Biomater 2011;99:142–9.
[29] Graham JS, Miron Y, Grandbois M. Structural changes in human type I collagen fibrils investigated by force spectroscopy. Exp Cell Res 2004;299:335–42.
[30] Pingarrón JM, Yáñez-Sedeño P, González-Cortés A. Gold nanoparticle-based electrochemical biosensors. Electrochem Acta 2008;53:5848–66.
[31] Cao X, Ye Y, Liu S. Gold nanoparticle-based signal amplification for biosensing. Anal Biochem 2011;417:1–16.
[32] Yeh YC, Creran B, Rotello VM. Gold nanoparticles: preparation, properties, and applications in bionanotechnology. Nanoscale 2012;4:1871–80.
[33] Hsu SH, Yen HJ, Tsai CL. The response of articular chondrocytes to type II collagen-Au nanocomposites. Artif Organs 2007;31:854–68.
[34] Brust M, Walker M, Bethell D, Schiffrin DJ, Whyman R. J Chem Soc Chem Commun 1994;3:801–2.
[35] Templeton AC, Chen S, Gross SM, Murray RW. Water-soluble, isolable gold clusters protected by tiopronin and coenzyme A monolayers. Langmuir 1998;15:66–76.
[36] Priyadarshini BM, Lu TB, Fawzy AS. Effect of photoactivated riboflavin on the biodegradation-resistance of root-dentin collagen. J Photochem Photobiol B 2017;177:18–23.
[37] Umer D, Yiu CK, Burrow MF, Niu LN, Tay FR. Effect of a novel quaternary ammonium silane on dentin protease activities. J Dent 2017;58:19–27.
[38] Seseogullari Dirihan R, Mutluay MM, Pashley DH, Tezvergil-Mutluay A. Is the inactivation of dentin proteases by crosslinkers reversible? Dent Mater 2017;33:e62–8.
[39] Fawzy AS, Nitisusanta L, Iqbal K, Daood U, Beng LT, Neo J. Characterization of riboflavin modified dentin collagen matrix. J Dent Res 2012;91:1049–54.
[40] Shiao-Wen T, Yi-Yun C, Jiunn-Woei L. Compound cellular imaging of laser scanning confocal microscopy by using gold nanoparticles and dyes. Sensors 2008;8:2306–16.
[41] Daood U, Yiu CKY. Transdentinal cytotoxicity and macrophage phenotype of a novel quaternary ammonium silane cavity disinfectant. Dent Mater 2019;35(2):206–16.
[42] Brown BN, Valentin JE, Stewart-Akers AM, McCabe GP, Badylak SF. Macrophage phenotype and remodeling outcomes in response to biologic scaffolds with and without a cellular component. Biomaterials 2009;30:1482–91.
[43] Tjäderhane L, Nascimento FD, Breschi L, Mazzoni A, Tersariol IL, Geraldeli S, et al. Optimizing dentin bond durability: control of collagen degradation by matrix metalloproteinases and cysteine cathepsins. Dent Mater 2013;29:116–35.
[44] Tjäderhane L. Dentin bonding: can we make it last? Oper Dent 2015;40:4–18.
[45] Sabatini C, Pashley DH. Mechanisms regulating the degradation of dentin matrices by endogenous dentin proteases and their role in dentin adhesion. A review. Am J Dent 2014;27:203–14.
[46] Daood U, Matinlinna JP, Fawzy AS. Synergistic effects of VE-TPGS and riboflavin in crosslinking of dentine. Dent Mater 2019;35(2):356–67.
[47] Agban Y, Lian J, Prabakar S, Seyfoddin A, Rupenthal ID. Nanoparticle cross-linked collagen shields for sustained delivery of pilocarpine hydrochloride. Int J Pharm 2016;501:96–101.
[48] Unser S, Holcomb S, Cary R, Sagle L. Collagen-gold nanoparticle conjugates for versatile biosensing. Sensors 2017;17:375.
[49] DeLong RK, Reynolds CM, Malcolm Y, Schaeffer A, Severs T, Wanekaya A. Functionalized gold nanoparticles for the binding, stabilization, and delivery of therapeutic DNA, RNA, and other biological macromolecules. Nanotechnol Sci Appl 2010;3:53.
[50] Olde Damink LHH, Dijkstra PJ, Van Luyn MJA, Van Wachem PB, et al. Glutaraldehyde as a crosslinking agent for collagen-based biomaterials. J Mater Sci Mater Med 1995;6:460–72.
[51] Castaneda M Valle J, Yang N, Pluskat S, Slowinska K. Collagen cross-linking with Au nanoparticles. Biomacromolecules 2008;9:3383–8.
[52] Shao Q, Hall CK. Binding preferences of amino acids for gold nanoparticles: a molecular simulation study. Langmuir 2016;32:7888–96.
[53] Bateman JF, Lamande S, Ramshaw JAM. Collagen superfamily. In: Comper WD, editor. Extracellular matrix: molecular components and interactions, Vol. 2. Amsterdam: Harwood Academic; 1995. p. 22–67.
[54] Pashley DH, Tay FR, Carvalho RM, Rueggeberg FA, Agee KA, Carrilho M, et al. From dry bonding to water-wet bonding to ethanol-wet bonding: a review of the interactions between dentin matrix and solvated resins using a macromodel of the hybrid layer. Am J Dent 2007;20:7–20.
[55] Seseogullari-Dirihan R, Apollonio F, Mazzoni A, Tjaderhane L, Pashley D, Breschi L, et al. Use of crosslinkers to inhibit dentin MMPs. Dent Mater 2016;32:423–32.
[56] Umer D, Yiu CKY, Burrow MF, Niu LN, Tay FR. Effect of a novel quaternary ammonium silane on dentin protease activities. J Dent 2017;58:19–27.
[57] Li Z, Hou WS, Escalante-Torres CR, Gelb BD, Bromme D. Collagenase activity of cathepsin K depends on complex formation with chondroitin sulfate. J Biol Chem 2002;277:28669–76.

[58] Seseogullari-Dirihan R, Mutluay MM, Tjaderhane L, Breschi L, Pashley DH, Tezvergil-Mutluay A. Effect of pH on dentin protease inactivation by carbodiimide. Eur J Oral Sci 2017;125:288–93.
[59] Nascimento FD, Minciotti CL, Geraldeli S, Carrilho MR, Pashley DH, Tay FR, et al. Cysteine cathepsins in human carious dentin. J Dent Res 2011;90:506–11.
[60] Lamparter S, Slight SH, Weber KT. Doxycycline and tissue repair in rats. J Lab Clin Med 2002;139:295–302.
[61] Williams RW. Estimation of protein secondary structure from the laser Raman amide I spectrum. J Mol Biol 1983;166:581–603.
[62] Goormaghtigh E, Cabiaux V, Ruysschaert JM. Secondary structure and dosage of soluble and membrane proteins by attenuated total reflection Fourier-transform infrared spectroscopy on hydrated films. Eur J Biochem 1990;193:409–20.
[63] Kadler K. The structure of collagens. Protein Profile 1995;2:508–23.
[64] Carden A, Rajachar R, Morris MD, Kohn D. Ultrastructural changes accompanying the mechanical deformation of bone tissue: a Raman imaging study. Calcif Tissue Int 2003;72:166–75.
[65] Paschalis EP, Tatakis DN, Robins S, Fratzl P, Manjubala I, Zoehrer R, et al. Lathyrism-induced alterations in collagen cross-links influence the mechanical properties of bone material without affecting the mineral. Bone 2011;49:1232–41.
[66] Stout RD, Jiang C, Matta B, Tietzel I, Watkins SK, Suttles J. Macrophages sequentially change their functional phenotype in response to changes in microenvironmental influences. J Immunol 2005;175:342–9.
[67] Andrade Jr I, Silva TA, Silva GA, Teixeira AL, Teixeira MM. The role of tumor necrosis factor receptor type 1 in orthodontic tooth movement. J Dent Res 2007;86:1089–94.